

INVESTIGATION OF $J \rightarrow J$ M1 TRANSITIONS IN ^{38}Ar

G. A. P. ENGELBERTINK, H. LINDEMAN[†] and M. J. N. JACOBS

Fysisch Laboratorium, Rijksuniversiteit, Utrecht, Nederland

Received 9 October 1967

Abstract: The γ -decay of eight $^{37}\text{Cl}(\text{p}, \gamma)^{38}\text{Ar}$ resonances in the range $E_p = 1.0$ – 1.8 MeV has been investigated with a 20 cm^3 Ge(Li) detector. Precision γ -ray energy measurements yield the energies of 23 bound states of ^{38}Ar (errors 0.14 – 3.0 keV) and the Q -value of the $^{37}\text{Cl}(\text{p}, \gamma)^{38}\text{Ar}$ reaction, $Q = 10\,242.5 \pm 1.1$ keV. Mean lifetimes (or lower limits) of 12 bound states were found from measurements of γ -ray Doppler shifts. The spins and parities of levels at $E_x = 4.57, 4.88, 5.51, 6.21, 6.60, 6.67, 11.35$ and 11.93 MeV have been determined as $J^\pi = (2^-), 3^-, 3^{(-)}, 4^-, 4^-, (5^-), 3^-$ and 4^- , respectively, on the basis of γ -ray angular-distribution and polarization measurements and/or intensity considerations. Several γ -ray multipole mixing ratios were obtained. The strong $J^\pi = 4^-$ resonance at $E_p = 1\,732$ keV can be regarded as the analogue of the third excited state in ^{38}Cl .

The strength of M1 transitions of $J \rightarrow J$ character, up to 0.4 – 0.6 W.u., is an order of magnitude larger than that of $J \rightarrow J \pm 1$ transitions.

NUCLEAR REACTIONS $^{37}\text{Cl}(\text{p}, \gamma)$, $E = 0.43, 1.0$ – 1.8 MeV; measured $\sigma(E; E_\gamma)$, Doppler-shift attenuation, $\text{p}, \gamma(\theta)$, γ -polarization. ^{38}Ar deduced levels, resonances, Q , branching, $J, \pi, T_{1/2}$, mixing ratios. Enriched target, Ge(Li) detector.

1. Introduction

Two of the many resonances in the $^{37}\text{Cl}(\text{p}, \gamma)^{38}\text{Ar}$ reaction have been studied by Ern  *et al.*¹⁾ These resonances at $E_p = 1\,089$ keV and $1\,094$ keV, both having $J^\pi = 5^-$, are the split analogue of $^{38}\text{Cl}(1)$.

The analogue of $^{38}\text{Cl}(2)$ with $J^\pi = 3^-$ has been reported in the work of Bošnjakovi  *et al.*²⁾ on the $^{37}\text{Cl}(\text{p}, \alpha_0)^{34}\text{S}$ reaction. This analogue appears to be split into at least seven components centered around $E_p = 1\,140$ keV.

This paper describes measurements on the γ -ray spectra of the strongest of these 3^- components at $E_p = 1\,138$ keV and of the analogue of $^{38}\text{Cl}(3)$ with $J^\pi = 4^-$, which was located at $E_p = 1\,732$ keV. The decay of the $J^\pi = 5^-$ analogue states has been re-investigated. From these measurements in combination with those on four other resonances at $E_p = 1\,136, 1\,142, 1\,262$ and $1\,320$ keV, the energies, branching ratios, lifetimes and J^π -values of many ^{38}Ar levels were determined.

Ern 's measurements on the $T=2, J^\pi=5^-$ analogue resonances showed that the decay mainly proceeds through strong M1 transitions to $T=1, J^\pi=5^-$ states. This can be understood¹⁾, if the main configurations of the odd-parity levels would have $d_{3/2}^{-1}f_{7/2}$

[†] On leave from the Technion-Israel Institute of Technology, Haifa, Israel.

character, and if the dominating part of the M1 operator operates on the particle in the $f_{7/2}$ shell.

One of the purposes of the present work was to investigate the strength of similar $4^- \rightarrow 4^-$ and $3^- \rightarrow 3^-$ M1 transitions.

2. Experimental procedure

The apparatus used to investigate (p, γ) reactions has been described previously by Van Rinsvelt and Smith ³). Protons from the Utrecht 3 MV van de Graaff accelerator pass through a 90° analysing magnet and a cooling trap ⁴) before hitting the target. The magnetic field of the analysing magnet is measured with an NMR fluxmeter.

The BaCl_2 targets enriched to 99% in ^{37}Cl , are evaporated onto tantalum backings. The backing forms part of the target holder such that it can be water cooled directly. The thickness of the targets varied between 0.8 and 5.0 keV for protons of 1 MeV.

Gamma radiation was detected with a 20 cm^3 Ge(Li) detector coupled to a 4096-channel Laben analyser. The resolution ranges from 6 keV at $E_\gamma = 1$ MeV to 18 keV at $E_\gamma = 9$ MeV. The γ -ray intensities were obtained from spectra recorded at $\theta = 55^\circ$, using the efficiency curve of this detector published by van der Leun *et al.* ⁵).

With a computer program, the peaks in the pulse-height spectra were fitted to Gaussian curves, from which the areas and the centra of the peaks were determined. The accuracy of the positions of the centre varied between 0.1 and 3 keV depending on the statistics obtained.

With a second computer program the peak positions were converted into energies. In this program the calibration curve (energy versus peak position) was developed in a power series.

The calibration curve is constructed in a least-squares procedure with the following constraints:

- (i) accurately known energies of peaks from radioactive sources and of the ever-present annihilation peak,
- (ii) the 511.006 keV distances between full-energy, single-escape and double-escape peaks and
- (iii) the requirement that the energies of the γ -rays emitted in cascades, after correction for recoil, should add up to the excitation energy of the resonance state.

Generally it was not necessary to take into account polynomials of a degree higher than three. The slope of the calibration curve deviates not more than about 1% from the mean slope. This alinearity of the system was mainly due to the pre-amplifier.

Energies of γ -rays were measured at $\theta = 90^\circ$ to avoid Doppler shifts.

Doppler shifts were measured by taking spectra at $\theta = 0^\circ$ and 140° and angular distributions at $\theta = 0^\circ, 35^\circ, 55^\circ$ and 90° .

In the yield and polarization measurements, two cylindrical NaI scintillation crystals, 10 cm long and 10 cm in diam., were used. The polarization measurements were performed with a Compton polarimeter as described by Suffert, Endt and Hoogenboom ⁶).

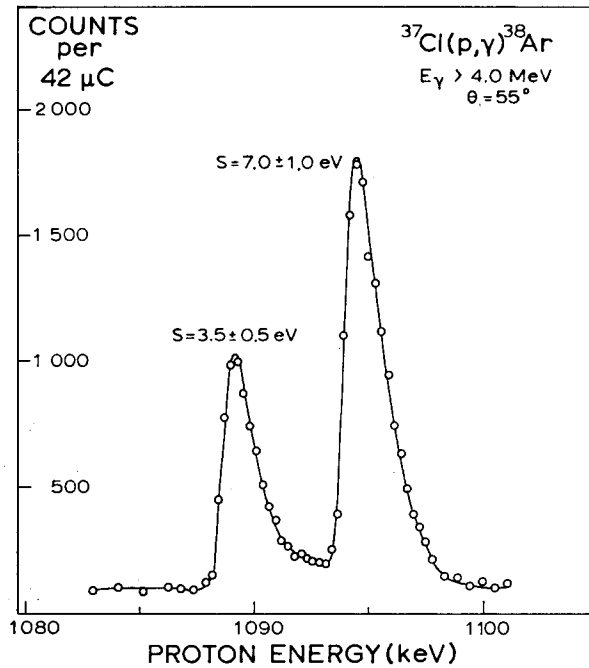


Fig. 1. Yield curve for the $^{37}\text{Cl}(p,\gamma)^{38}\text{Ar}$ reaction indicating the $E_p = 1089$ and 1094 keV resonances. The target distance to front of NaI crystal is 4 cm.

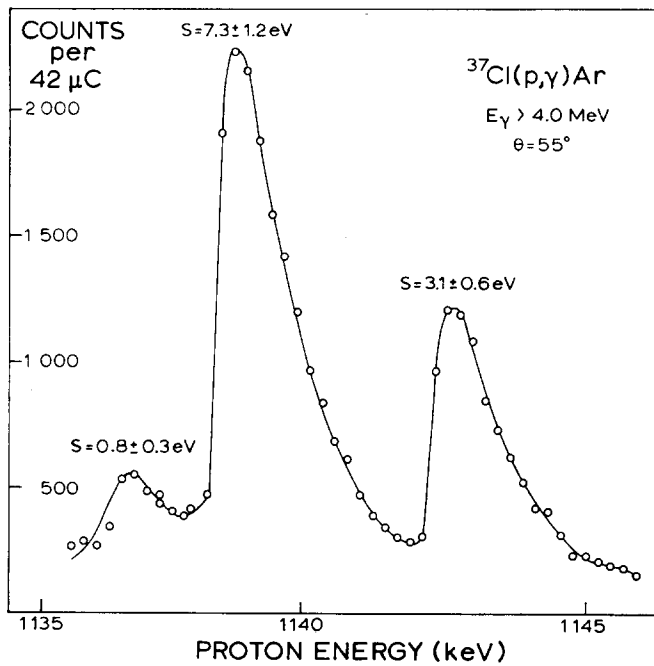


Fig. 2. Yield curve for the $^{37}\text{Cl}(p,\gamma)^{38}\text{Ar}$ reaction indicating the $E_p = 1136$, 1138 and 1142 keV resonances. The target distance to front of NaI crystal is 4 cm.

3. Results

3.1. YIELDS, ENERGIES AND DECAY MODES OF THE RESONANCES

Gamma-ray yield curves were measured at 55° with two discriminator channels ($E_\gamma > 2.0$ MeV and > 4.0 MeV) and targets of about 2 keV thickness. The distance between the target and the front of the NaI crystal was 4 cm. The yield curve in the regions of the $E_p = 1\,089$ and $1\,094$, $1\,138$ and $1\,732$ keV resonances is shown in figs. 1-3.

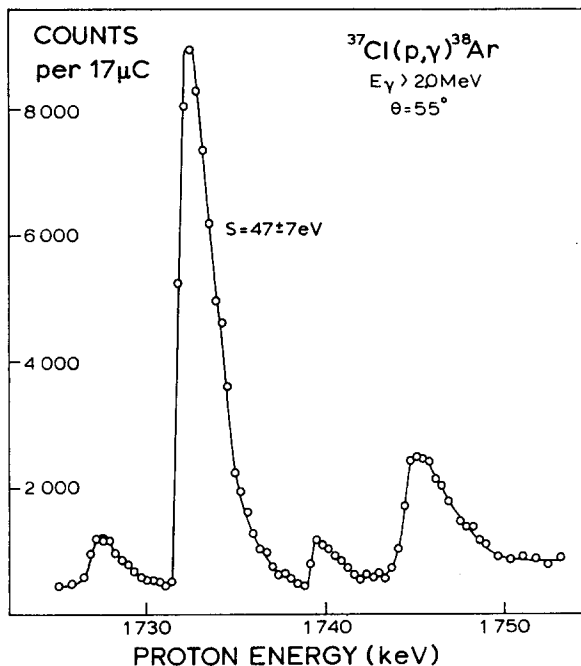


Fig. 3. Yield curve for the $^{37}\text{Cl}(p,\gamma)^{38}\text{Ar}$ reaction indicating the $E_p = 1\,732$ keV resonance. The other three resonances are not discussed in the present work. The target distance to front of NaI crystal is 4 cm.

The strengths of these analogue resonances were determined by relative measurements ⁷⁾ (with the same target) in which the resonance at $E_p = 847$ keV, $S = (2J+1)\Gamma_p\Gamma_\gamma/\Gamma = 1.04 \pm 0.15$ eV was used as a standard. The strengths of the other resonances were measured relative to those of this primary set of four. The results are given in fig. 4.

The energies of the analogue resonances were determined by comparison with the standard $^{27}\text{Al}(p,\gamma)^{28}\text{Si}$ resonance at $E_p = 991.87 \pm 0.06$ keV [ref. ⁸⁾]. A relativistic correction for the proton energy was applied ³⁾. The energies of the other resonances were measured relative to those of the analogue resonances. The results are also given in fig. 4.

The γ -ray spectra of the $E_p = 1\,089$, $1\,138$ and $1\,732$ keV analogue states are shown in figs. 5-7 and the corresponding decay schemes in figs. 5a, 6a and 7a. The decay of the $E_p = 1\,094$ keV state is very similar to that of the $E_p = 1\,089$ keV resonance (see fig. 4).

GAMMA RAY BRANCHINGS ^{38}Ar

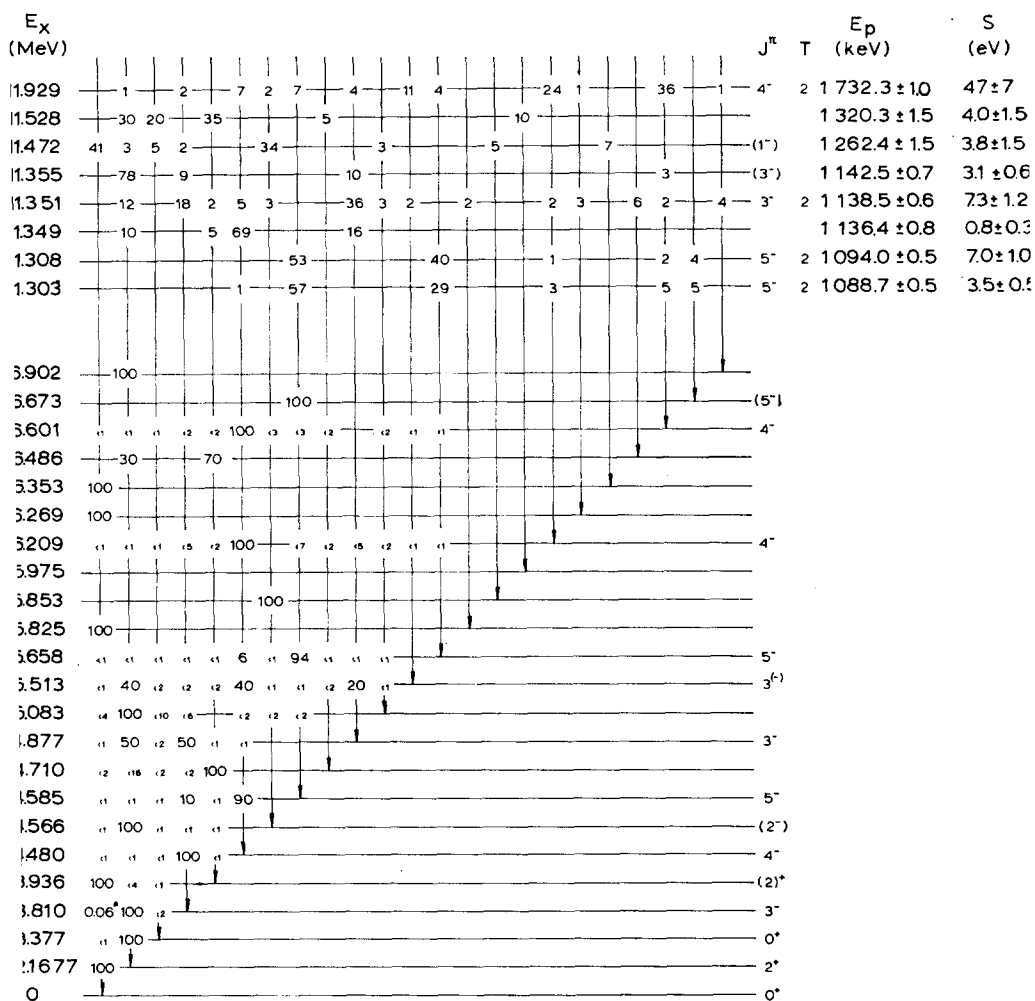


Fig. 4. Branching ratios of resonance levels and bound states in ^{38}Ar ; resonance energies and strengths.

* The entry marked with an asterisk is taken from ref. ²⁴).

The decay modes of the four analogue states and those of the four other resonances studied are given in fig. 4. The high γ -ray energy resolution enables a detailed analysis of the decay of the resonance states, such that measurements of coincidence

counts in the calibration peaks was about the same as that in the stronger peaks of the spectrum. A typical example is shown in fig. 8. The energy dispersion in these measurements varied between 0.7 and 1.5 keV per channel.

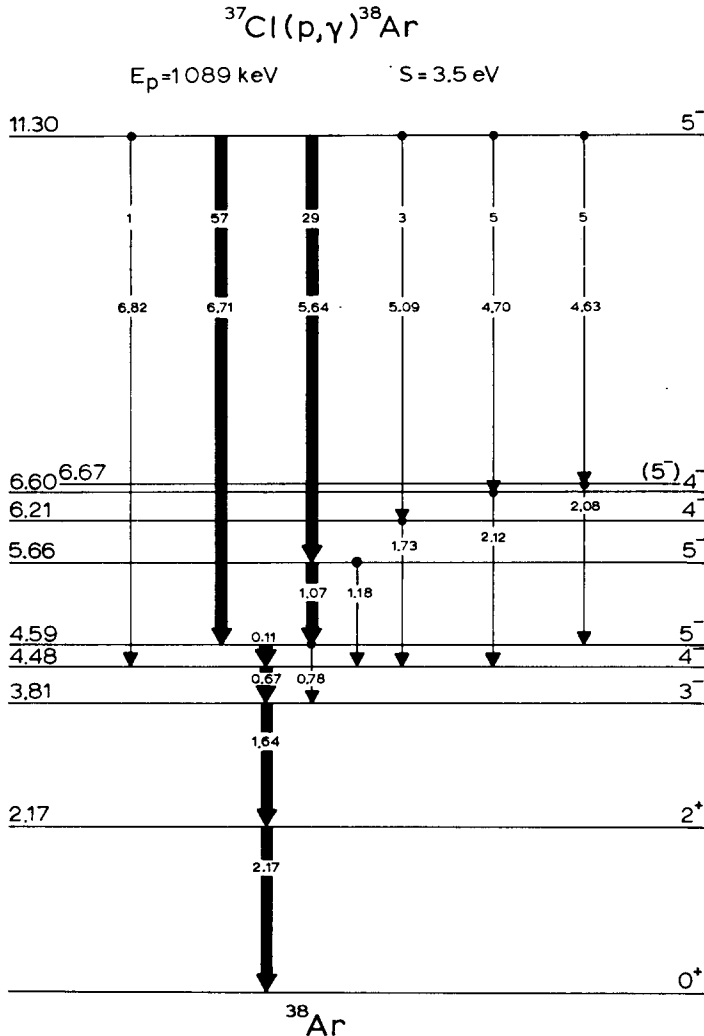


Fig. 5(a). Decay scheme corresponding to the spectrum shown in fig. 5.

The calibration curve was constructed from the peaks of the radioactive sources, the annihilation peak and the 511.006 keV escape peak distances. The energies of the γ -rays emitted by the radioactive sources have been taken from ref. ⁹).

The energies thus found for 15 γ -rays, all with $E_\gamma < 4.0 \text{ MeV}$, are presented in table 1. From them, after recoil correction, the excitation energies of 13 ^{38}Ar levels were obtained with errors below 0.8 keV. These are given in table 7.

Some ten more ^{38}Ar excitation energies with errors up to 3 keV, also appearing in table 7, could be found with the additional aid of the reaction Q -value ($Q = 10242.5 \pm 1.1$ keV, see below), on the basis of the requirement that the energies of the

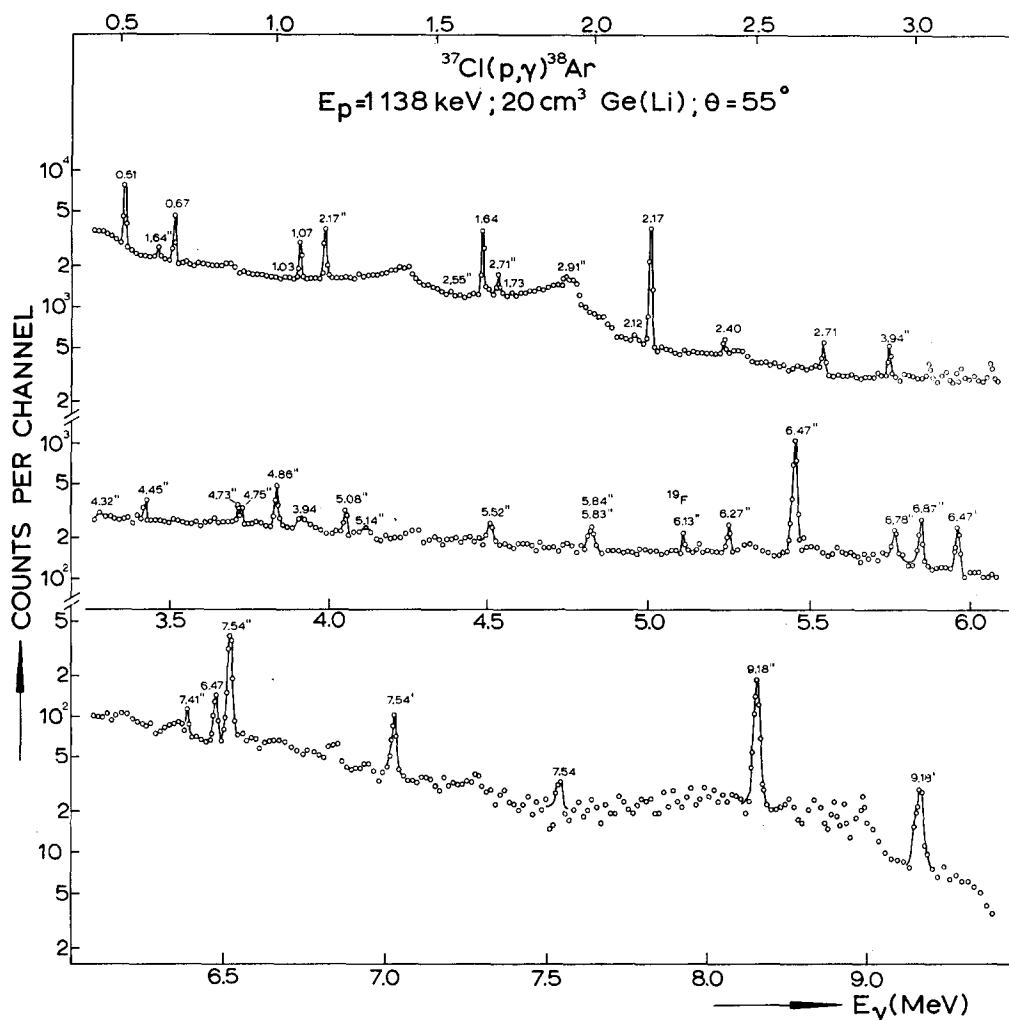


Fig. 6. Gamma-ray spectrum at the $E_p = 1138$ keV $^{37}\text{Cl}(p, \gamma)^{38}\text{Ar}$ resonance taken with a 20 cm^3 Ge(Li) detector at a distance of 4 cm and an angle $\theta = 55^\circ$ to the beam direction. For notation, see caption of fig. 5.

γ -rays emitted in cascades (after correction for recoil) should add up to the excitation energy of the resonance state (see sect. 2).

In column 4 of table 7, excitation energies are compared with previous results from the $^{41}\text{K}(p, \alpha)^{38}\text{Ar}$ reaction¹⁰).

The reaction Q -value has been obtained from the spectrum at the $1\,088.7 \pm 0.5$ keV resonance. This spectrum shows the 6.13 MeV γ -ray, due to the background reaction $^{19}\text{F}(p, \alpha\gamma)^{16}\text{O}$ with the known 9) energy of $6\,129.3 \pm 0.4$ keV.

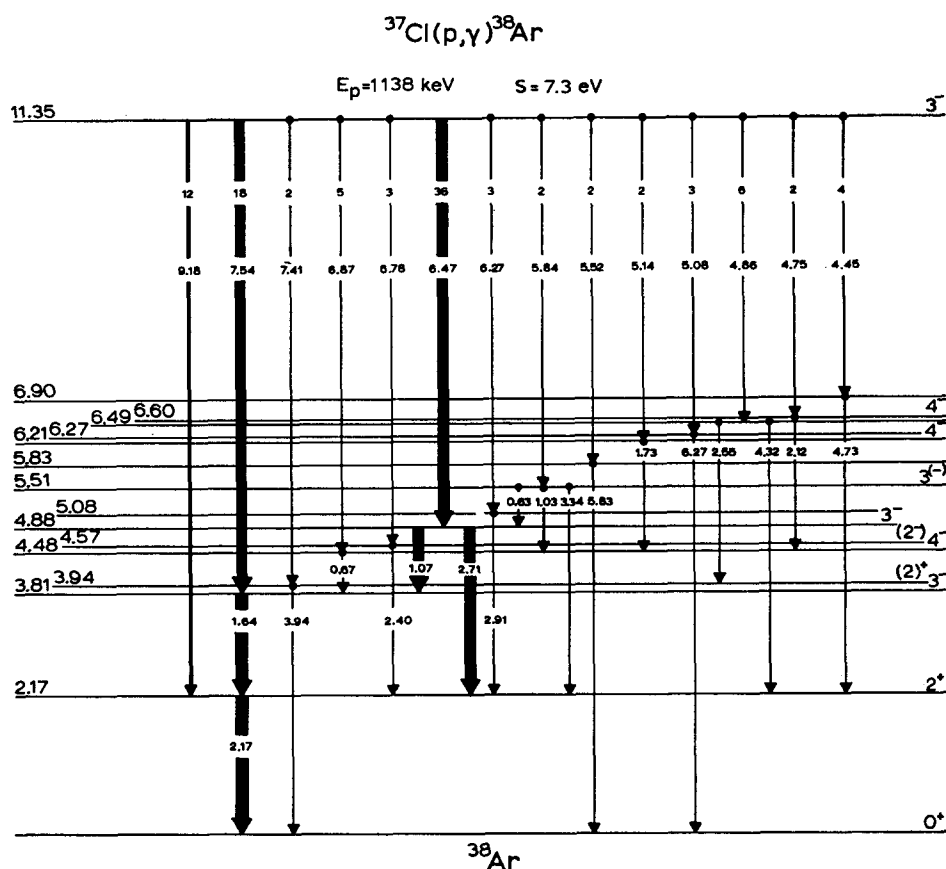


Fig. 6(a). Decay scheme corresponding to the spectrum shown in fig. 6.

The difference between the 6.13 MeV double-escape peak and the 5.64 MeV single-escape peak of the transition feeding the 5.66 MeV level is about 25 keV, which enables an accurate γ -ray energy measurement (see fig. 9). The result is $E_\gamma = 5\,644.3 \pm 0.8$ keV.

From this value (after recoil correction) in combination with the excitation energy of the 5.66 MeV level (table 7) and the resonance proton energy, the Q -value for the $^{37}\text{Cl}(p, \gamma)^{38}\text{Ar}$ reaction is found as $Q = 10\,242.5 \pm 1.1$ keV. This result is in excellent agreement with (but more accurate than) the value given in the 1964 mass table ¹¹⁾, $Q = 10\,242.4 \pm 2.3$ keV.

3.3. LIFETIMES OF BOUND STATES

The high resolution of the Ge(Li) detector made it also possible to measure Doppler shifts, although the shifts at these low proton bombarding energies are small. For short-lived states, the shift amounts to $\Delta E_\gamma/E_\gamma = 1.73 \times 10^{-3}$ at $E_p = 2$ MeV.

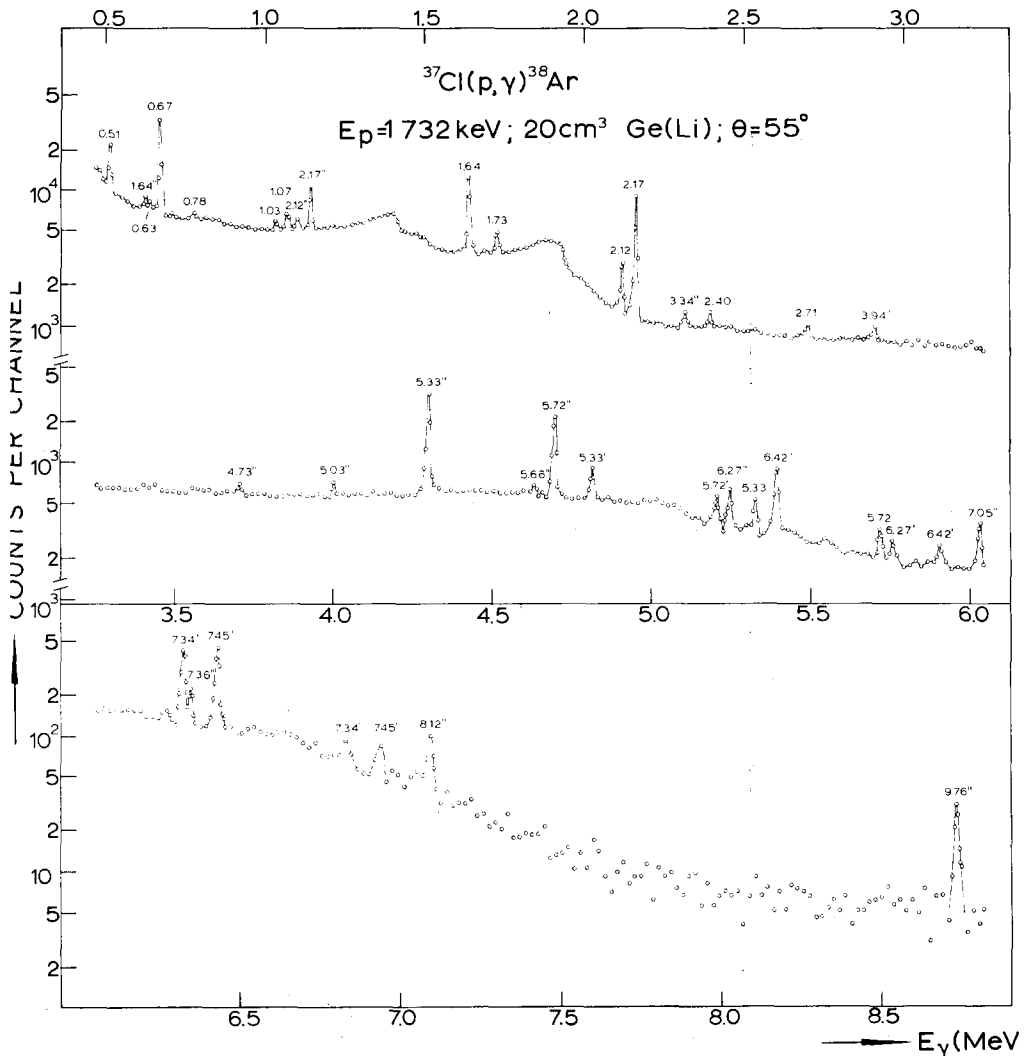


Fig. 7. Gamma-ray spectrum at the $E_p = 1732$ keV $^{37}\text{Cl}(p, \gamma)^{38}\text{Ar}$ resonance taken with a 20 cm^3 Ge(Li) detector at a distance of 4 cm and at an angle $\theta = 55^\circ$ to the beam direction. For notation, see caption of fig. 5.

Because of the low initial velocity of the ^{38}Ar ions ($v/c \approx 0.002$), the stopping process takes place in the target material, and the specific energy loss due to the

atomic collisions dominates the electronic part. The specific energy loss function was given by Lindhard *et al.* ¹²⁾ and the appropriate formulae (including direction straggling) for the evaluation of Doppler shifts by Blaugrund ¹³⁾.

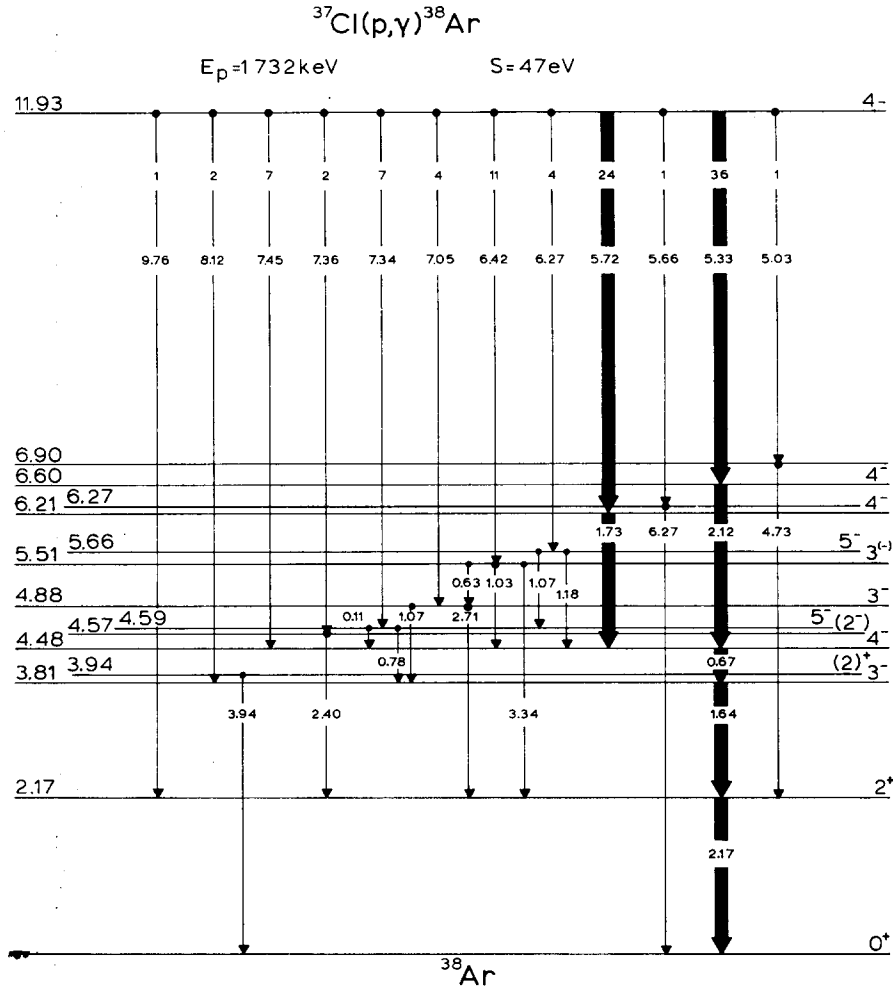


Fig. 7(a). Decay scheme corresponding to the spectrum shown in fig. 7.

For the atomic energy loss function $(d\varepsilon/d\rho)_n$ [notation of ref. ¹³⁾], the following expression was used:

$$\left(\frac{d\varepsilon}{d\rho}\right)_n = -c \log \left(\frac{\varepsilon^\alpha}{a} + \frac{b}{\varepsilon^\beta} \right),$$

with $c = 0.200$, $\alpha = 1.215$, $a = 70.0$, $b = 0.00200$ and $\beta = 0.815$. In the dimension-

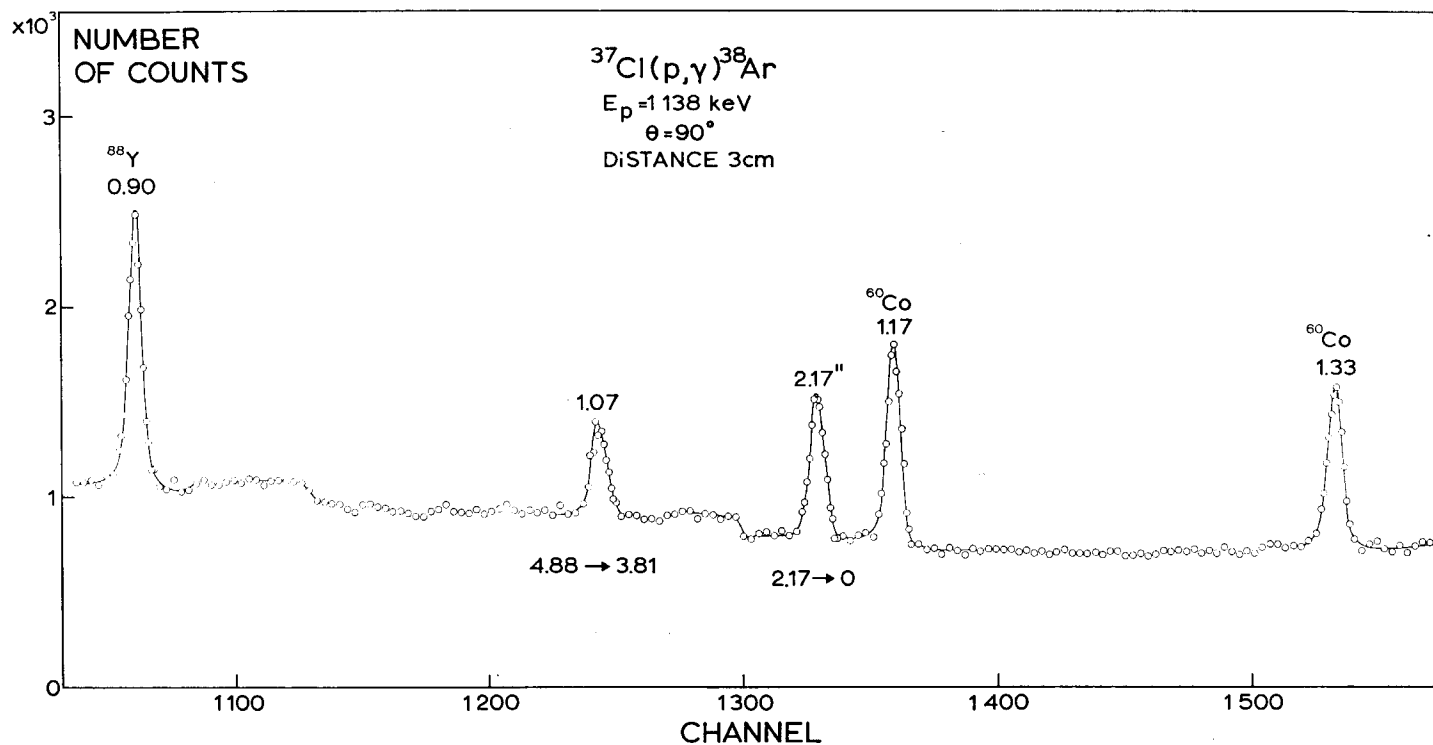


Fig. 8. Measurement of γ -ray energies in the $^{37}\text{Cl}(p,\gamma)^{38}\text{Ar}$ reaction. The figure shows part of the γ -ray spectrum at the $E_p = 1\,138\text{ keV}$ resonance together with γ -rays of the radioactive sources ^{88}Y and ^{60}Co taken with a $20\text{ cm}^3\text{ Ge(Li)}$ detector at $\theta = 90^\circ$ and at a distance of 3 cm from the target. For notation, see caption of fig. 5.

less energy range $2 \times 10^{-3} \leq \varepsilon \leq 10$, this function fits the curve given by Lindhard to within 2 %.

For the electronic loss function $(d\varepsilon/d\rho)_e$ the expression $(d\varepsilon/d\rho)_e = k\sqrt{\varepsilon}$ is given by Lindhard *et al.* ¹²⁾ with

$$k = 0.0793 \xi_e \frac{Z_1^{\frac{1}{2}} Z_2^{\frac{1}{2}} (A_1 + A_2)^{\frac{1}{2}}}{(Z_1^{\frac{1}{2}} + Z_2^{\frac{1}{2}})^{\frac{1}{2}} A_1^{\frac{1}{2}} A_2^{\frac{1}{2}}},$$

where $\xi_e = Z_1^{\frac{1}{2}}$. It is seen that the remaining part of the expression for k is symmetric in Z_1 (projectile) and Z_2 (stopping material).

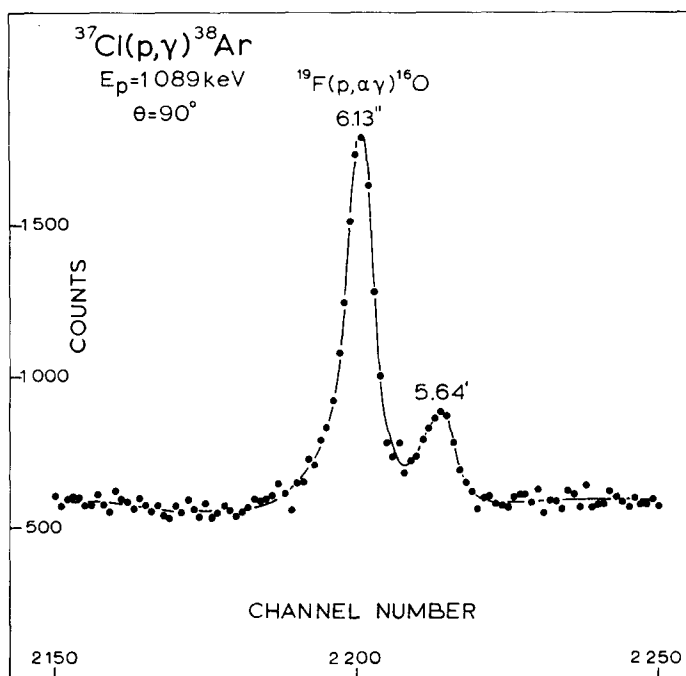


Fig. 9. Energy measurement of the 5.64 MeV γ -ray at the $E_p = 1089$ keV resonance of the $^{37}\text{Cl}(p, \gamma)^{38}\text{Ar}$ reaction. The figure shows the part of the spectrum which contains the 5.64 MeV single-escape peak and the 6.13 MeV double-escape peak due to the background reaction $^{19}\text{F}(p, \alpha\gamma)^{16}\text{O}$, of which the energy is known as 6129.3 ± 0.4 keV.

However, from the work of Ormrod *et al.* ¹⁴⁾ it appears that the electronic stopping cross section is not exactly described by Lindhard's formula, but that it shows oscillations around the Lindhard curve. The difference depends on Z_1 and is independent of Z_2 . The amplitude amounts to about 30 % of the Lindhard estimate. In the present computations, this periodic variation has been taken into account.

The γ -ray spectra at $\theta = 0^\circ$ and 140° taken for the measurement of the Doppler shifts were stored in the two 2048-channel halves of the pulse-height analyser. The distance between target and detector was 5 cm. The measurements were performed

with relatively thick targets (between 18 and 35 $\mu\text{g}/\text{cm}^2$) to make sure that the ^{38}Ar ions were stopped in the target layer and not partly in the backing.

The composition of the targets (1 Ba atom against 2 atoms ^{37}Cl) was checked with the $^{37}\text{Cl}(p, p)^{37}\text{Cl}$ reaction¹⁵).

The measurements at the two angles were carried out in many short (15 min) runs as a precaution against gain drifts. The target room was temperature controlled, but no special gain stabilization was used.

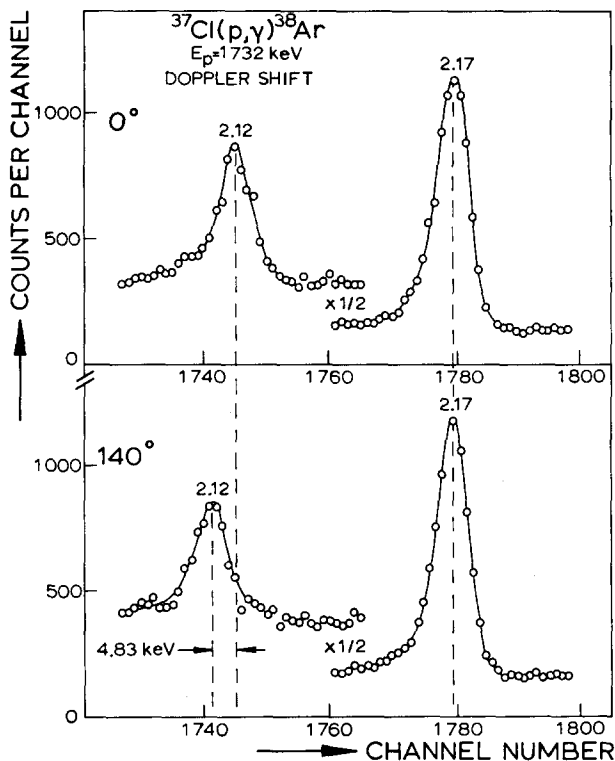


Fig. 10. Doppler-shift measurement for the peaks at 2.12 MeV and 2.17 MeV in the spectrum of the $E_p = 1732$ keV resonance. The spectra are taken at a distance of 5 cm and at angles $\theta = 0^\circ$ and $\theta = 140^\circ$. The 2.12 MeV peak shows a shift of 4.8 keV, which corresponds to 80 % of the full shift.

For the 2.17 MeV peak no shift is observed within the experimental error.

The energy dispersion used in these measurements varied between 0.7 and 1.5 keV per channel. An illustrative example of the results obtained is given in fig. 10.

The lifetimes of the resonance levels, all being smaller than 1 fs, could be neglected.

No correction was needed for the recoil caused by the primary γ -rays, because the angular distribution is symmetric around $\theta = 90^\circ$. A correction was applied, if the level in question was also excited in a cascade through a higher level with previously measured mean life.

TABLE 1
Gamma-ray energies from the $^{37}\text{Cl}(\text{p}, \gamma)^{38}\text{Ar}$ reaction at $\theta = 90^\circ$

E_γ ^{a)} (keV)	Assignment (E_x in ^{38}Ar in keV)
105.5 \pm 0.4	4 585 \rightarrow 4 480
669.58 \pm 0.14 ^{b)}	4 480 \rightarrow 3 810
773.3 \pm 0.5	4 711 \rightarrow 3 938
774.9 \pm 0.5	4 585 \rightarrow 3 810
1 033.3 \pm 0.4	5 513 \rightarrow 4 480
1 066.8 \pm 0.3	4 877 \rightarrow 3 810
1 072.7 \pm 0.3	5 658 \rightarrow 4 585
1 209.1 \pm 0.3	3 377 \rightarrow 2 168
1 642.31 \pm 0.14 ^{b)}	3 810 \rightarrow 2 168
1 729.4 \pm 0.6	6 209 \rightarrow 4 480
2 121.55 \pm 0.21	6 601 \rightarrow 4 480
2 167.61 \pm 0.14 ^{b)}	2 168 \rightarrow 0
2 398.1 \pm 0.5	4 566 \rightarrow 2 168
2 709.4 \pm 0.4	4 877 \rightarrow 2 168
3 936.1 \pm 0.5	3 936 \rightarrow 0

^{a)} Not corrected for recoil losses. The quoted error is equal to the internal or external error, whichever is the larger.

^{b)} Weighted mean of eight measurements at different resonances.

TABLE 2
Values or limits for the mean lifetime of ^{38}Ar levels

E_x (MeV)	Decay to (E_x in MeV)	E_p ^{a)} (keV)	F ^{b)}	τ_m ^{c)} (fs)
2.17	0	1 142	0.01 \pm 0.03	\geq 1000
3.38	2.17	1 320	0.03 \pm 0.05	\geq 500
3.81	2.17	1 138	0.40 \pm 0.12	110 \pm 80
3.94	0	1 320	0.43 \pm 0.04	105 \pm 16
4.48	3.81	1 136	0.02 \pm 0.05	\geq 600
4.57	2.17	1 262	0.62 \pm 0.05	48 \pm 10
4.59	3.81	1 089	0.02 \pm 0.05	\geq 500
4.88	2.17	1 138	0.68 \pm 0.10	39 \pm 13
	3.81	1 138	0.65 \pm 0.11	
5.51	2.17	1 732	0.00 \pm 0.10	\geq 300
5.66	4.59	1 089	0.54 \pm 0.06	64 \pm 14
6.21	4.48	1 732	0.50 \pm 0.07	90 \pm 25
6.60	4.48	1 732	0.80 \pm 0.04	25 \pm 7

^{a)} The proton energy of the resonance in the decay of which the transition is observed.

^{b)} Ratio between the measured shift, and the full shift (for an infinitely short-lived level). The stopping material is in all cases $\text{Ba}^{37}\text{Cl}_2$.

^{c)} Lower limits correspond to the measured F -value plus two times the standard deviation.

The measured Doppler shift F , as a fraction of the full shift, is presented in fig. 11 as a function of the mean life τ_m for three values of the proton energy.

Errors due to uncertainties in the stopping theory are not taken into account, i.e. the curve in fig. 11 is considered as being correct. These uncertainties are estimated by Lindhard *et al.* ¹²⁾ to be about 20 %. They may even be more, because of the low recoil velocities which occur in these Doppler-shift experiments.

The measured shifts and the mean lives computed from them are given in table 2.

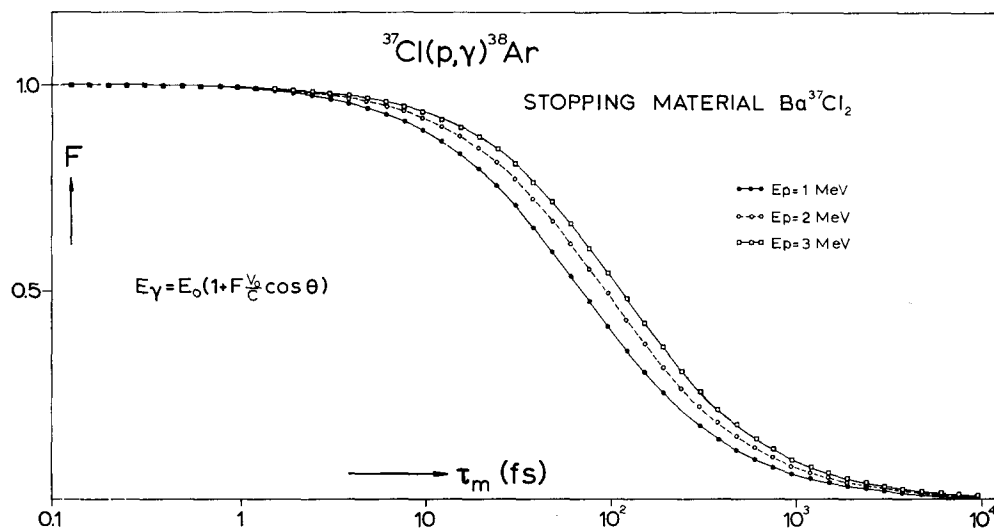


Fig. 11. The Doppler shift expressed as a fraction F of the full shift, as a function of the mean life τ_m , computed from the theory mentioned in subject. 3.3.

3.4. SPINS AND PARITIES

In this section it will be shown how the spins and parities of the 11.35 and 11.93 MeV resonance levels and of some lower levels were determined from angular-distribution and polarization measurements in combination with the yield and life-time measurements reported in subjects. 3.1 and 3.3. Where intensity considerations had to be applied in rejecting certain J^π and/or x -values, the upper limits for the strengths of possible E2 and M2 transitions were taken as 10 W.u. in consideration of the fact that the mixing ratios found by Ern  ¹⁾ indicate low E2 strengths.

Angular distributions were measured for several γ -rays at the $E_p = 1\,089$, $1\,138$ and $1\,732$ keV resonances by taking Ge(Li) spectra at $\theta = 0^\circ, 35^\circ, 55^\circ$ and 90° at 3 or 4 cm distance from the target. The distributions were expanded in a Legendre polynomial series

$$W(\theta) \propto 1 + A_2 P_2(\cos \theta) + A_4 P_4(\cos \theta),$$

where θ is the angle between the γ -ray and the direction of the proton beam. The

error in the measured coefficients A_2 and A_4 depends on the intensity of the particular γ -ray and amounts for strong lines to about 0.02.

The linear polarization of the most prominent γ -rays emitted at 90° to the proton beam was determined with a NaI Compton polarimeter as described by Suffert *et al.*⁶⁾. The measured effect is expressed in the quantity $pP = (N_0 - N_{90})/(N_0 + N_{90})$ where N_{90} and N_0 are the intensities observed at 90° and 0° , p the polarization efficiency of the polarimeter and P the polarization. The 90° direction lies in the plane perpendicular to the proton beam.

The results of the above measurements are presented in table 3. For the $E_p = 1\,089$ keV resonance, only the data additional to those of ref. ¹⁾ are given, because the results for the other γ -rays agreed within the experimental errors with the values given there.

TABLE 3

Results from angular-distribution and polarization measurements at the $E_p = 1\,089$, $1\,138$ and $1\,732$ keV resonances

E_γ (MeV)	Transition (E_x in MeV)	Angular-distribution coefficients		Polarization P
		A_2	A_4	
1 089 keV <i>resonance</i> ^{a)}				
0.78	4.59 \rightarrow 3.81	$+0.31 \pm 0.06$	-0.06 ± 0.06	
1.18	5.66 \rightarrow 4.48	-0.40 ± 0.20	-0.03 ± 0.22	
4.63	11.30 \rightarrow 6.67	$+0.40 \pm 0.10$	$+0.11 \pm 0.10$	
4.70	11.30 \rightarrow 6.60	-0.30 ± 0.10	$+0.10 \pm 0.11$	
5.09	11.30 \rightarrow 6.21	-0.30 ± 0.20	$+0.15 \pm 0.22$	
1 138 keV <i>resonance</i>				
1.07	4.88 \rightarrow 3.81	$+0.32 \pm 0.07$	-0.01 ± 0.07	-0.18 ± 0.05
1.64	3.81 \rightarrow 2.17	-0.10 ± 0.03	-0.02 ± 0.03	
2.17	2.17 \rightarrow 0	$+0.11 \pm 0.03$	-0.01 ± 0.03	
2.71	4.88 \rightarrow 2.17	-0.01 ± 0.09	-0.01 ± 0.09	
6.47	11.35 \rightarrow 4.88	$+0.20 \pm 0.05$	$+0.02 \pm 0.05$	-0.15 ± 0.07
7.54	11.35 \rightarrow 3.81	$+0.16 \pm 0.06$	-0.05 ± 0.06	
9.18	11.35 \rightarrow 2.17	-0.30 ± 0.02	$+0.01 \pm 0.02$	
1 732 keV <i>resonance</i>				
0.67	4.48 \rightarrow 3.81	-0.14 ± 0.02	-0.03 ± 0.02	
1.03	5.51 \rightarrow 4.48	$+0.37 \pm 0.07$	-0.07 ± 0.07	
1.64	3.81 \rightarrow 2.17	-0.05 ± 0.02	-0.03 ± 0.02	
1.73	6.21 \rightarrow 4.48	-0.03 ± 0.04	-0.06 ± 0.04	
2.12	6.60 \rightarrow 4.48	$+0.22 \pm 0.03$	-0.06 ± 0.04	
2.17	2.17 \rightarrow 0	$+0.23 \pm 0.02$	-0.02 ± 0.02	
3.34	5.51 \rightarrow 2.17	-0.32 ± 0.10	$+0.07 \pm 0.10$	
5.33	11.93 \rightarrow 6.60	$+0.31 \pm 0.02$	$+0.04 \pm 0.03$	-0.35 ± 0.18
5.72	11.93 \rightarrow 6.21	$+0.28 \pm 0.03$	$+0.01 \pm 0.03$	-0.65 ± 0.30
6.42	11.93 \rightarrow 5.51	-0.24 ± 0.04	$+0.01 \pm 0.04$	
7.34	11.93 \rightarrow 4.59	$+0.14 \pm 0.04$	$+0.05 \pm 0.05$	
7.45	11.93 \rightarrow 4.48	$+0.24 \pm 0.05$	$+0.05 \pm 0.05$	

^{a)} Data additional to those of ref. ¹⁾.

The experimental values of the A_2 and A_4 coefficients and the polarization P were compared with the theoretical values ¹⁶⁾ by a least-squares procedure for all possible spin combinations.

In the computer program used for this purpose, all the relevant parameters of a cascade, i.e. quadrupole/dipole or octupole/quadrupole mixing parameters x and formation parameters (statistical tensors) ρ_{k0} were varied in small steps and a χ^2 -value was calculated for each combination of the parameters.

Limiting values are imposed on the statistical tensors from the requirement that the population probabilities of magnetic substates are non-negative.

3.4.1. *The $E_p = 1\,732$ keV resonance; the 5.51, 6.21 and 6.60 MeV levels.* The analysis of the $E_p = 1\,732$ keV ($E_x = 11.93$ MeV) resonance proceeds as follows.

The radiation strength of the resonance and the lifetimes of the 6.21 and 6.60 MeV levels exclude pure quadrupole radiation for the 5.33 ($r \rightarrow 6.60$), 5.72 ($r \rightarrow 6.21$), 2.12 (6.60 \rightarrow 4.48) and 1.73 (6.21 \rightarrow 4.48) MeV γ -rays.

A fit to the measured values of A_2 (5.33), A_4 (5.33), P (5.33), A_2 (2.12) and A_4 (2.12) as outlined above with the restriction that quadrupole admixtures exceeding 10 W.u. are excluded, gives as possible spin and parity combinations $J^\pi(11.93) = J^\pi(6.60) = 3^\pm, 4^\pm$ or 5^\pm .

All other spin and parity possibilities lead to a χ^2 -value above the 0.1 % confidence limit.

The same procedure used for the 11.93 \rightarrow 6.21 \rightarrow 4.48 MeV cascade yields $J^\pi(11.93) = J^\pi(6.21) = 3^\pm, 4^\pm$ or 5^\pm .

The combined result is $J^\pi(11.93) = J^\pi(6.60) = J^\pi(6.21) = 3^\pm, 4^\pm$ or 5^\pm .

A further restriction of the possible J -values is obtained from an angular-distribution measurement at the $E_p = 1\,089$ keV resonance [$J^\pi = 5^-$, see ref. ¹⁾]. The 5 % branch from the resonance level to the 6.60 MeV level ($E_\gamma = 4.70$ MeV) shows an angular-distribution coefficient $A_2 = -0.30 \pm 0.10$. Assuming $J(6.60) = 3$, one computes for the angular distribution of this pure quadrupole transition $A_2 = +0.28$ (the measured resonance strength forbids appreciable octupole admixture). Thus, the possibility of $J^\pi(11.93) = J^\pi(6.60) = J^\pi(6.21) = 3^\pm$ is excluded.

If the resonance level would have $J^\pi = 5^-$, the only formation possibility would be f -capture via channel spin 2. This implies a value for the statistical-tensor ratio of $\rho_{20}/\rho_{00} = -0.981$. The value of this ratio found from the least-squares procedure is $\rho_{20}/\rho_{00} = -0.64 \pm 0.05$, which rules out the 5^- possibility.

A value $J^\pi(11.93) = 5^+$ would involve an M2 strength of at least 18 W.u. for the $E_\gamma = 8.12$ MeV, 11.93 \rightarrow 3.81 MeV transition.

Thus, the remaining possibilities are $J^\pi(11.93) = J^\pi(6.60) = J^\pi(6.21) = 4^\pm$, with the following values for the continuous parameters: $\rho_{20}/\rho_{00} = -0.65 \pm 0.05$, $\rho_{40}/\rho_{00} = 0.0 \pm 0.2$, $x(5.33) = -0.05 \pm 0.08$, $x(5.72) = +0.02 \pm 0.08$, $x(2.12) = +0.05 \pm 0.08$, $x(1.73) = +0.32 \pm 0.10$.

The parity of the three levels can be proven to be odd in two different ways.

(i) The mixing ratio of the 1.73 MeV γ -ray implies, for $J^\pi(6.21) = 4^+$, an M2 strength of at least 270 W.u. This excludes even parity for the 6.21 MeV level.

(ii) For $J^\pi(11.93) = 4^+$, the formation of this level can occur via channel spin 1 with $l_p = 4$ and channel spin 2 with $l_p = 2$ and $l_p = 4$. A continuum of solutions exists reproducing the value $\rho_{20}/\rho_{00} = -0.65 \pm 0.05$.

The solution with the smallest amount of g -capture occurs for $\tau = 0$, $\varepsilon = 1.0$, with the channel spin mixing ratio τ defined as the intensity in the lowest spin channel over the total intensity in both channels, and the orbital momentum mixing ratio ε as the ratio of the higher orbital momentum amplitude to the lower one. This value of ε would correspond to at least 21 % of the Wigner limit for g -capture, which is improbable for a non-analogue resonance.

We thus can conclude to the unique assignments $J^\pi(11.93) = J^\pi(6.60) = J^\pi(6.21) = 4^-$.

Excluding pure octupole transitions, the spin of the 5.51 MeV level is limited to the values 2, 3 or 4 by the observation of the 11.93 \rightarrow 5.51 \rightarrow 2.17 MeV cascade. A simultaneous least-squares fit to the angular distributions of the 6.42 ($r \rightarrow 5.51$), 3.34 (5.51 \rightarrow 2.17) and 1.03 (5.51 \rightarrow 4.48) MeV γ -rays yields a unique solution $J(5.51) = 3$. The preferential decay of the analogue states to odd-parity levels suggests odd parity for the 5.51 MeV level.

The $J^\pi(11.93) = 4^-$ resonance level can only be formed by pure f -capture, because more than 6 % h -capture would already exceed the Wigner limit. The value obtained for ρ_{20}/ρ_{00} determines the channel spin ratio as $\tau = 0.05 \pm 0.10$.

From the resonance strength a lower limit for the proton width can be given as $\Gamma_p \geq 5.2$ eV, which involves $\theta_p^2 \geq 0.016$ for the reduced width.

Summary of results

$J^\pi(11.93) = J^\pi(6.60) = J^\pi(6.21) = 4^-$, $\rho_{20}/\rho_{00} = -0.65 \pm 0.05$, $\rho_{40}/\rho_{00} = 0.0 \pm 0.2$, $x(11.93 \rightarrow 6.21) = +0.02 \pm 0.08$, $x(11.93 \rightarrow 6.60) = -0.05 \pm 0.08$, $x(6.60 \rightarrow 4.48) = +0.05 \pm 0.08$, $x(6.21 \rightarrow 4.48) = +0.32 \pm 0.10$, $J(5.51) = 3^{(-)}$; formation: pure f -capture, $\tau = 0.05 \pm 0.10$.

3.4.2. *The $E_p = 1\,138$ keV resonance and the 4.88 MeV level.* The analysis of the $E_p = 1\,138$ keV resonance proceeds in a similar way. One excludes $J(11.35) = 5$ for the resonance level because it decays with a strong transition to the 2.17 MeV ($J^\pi = 2^+$) level; $J^\pi(11.35) = 4^-$ would involve for the same transition an M2 strength of at least 12 W.u.; $J^\pi(11.35) = 2^+$ involves for the 6.87 MeV (11.35 \rightarrow 4.48 MeV) γ -ray an M2 strength of at least 20 W.u.

Assuming $J^\pi(11.35) = 4^+$ and taking into account all formation possibilities (by variation of the orbital-momentum and channel spin mixing parameters), the values obtained for the statistical-tensor ratio are all within the range $\rho_{20}/\rho_{00} < -0.60$. This implies for the A_2 coefficient of the 11.35 \rightarrow 2.17 MeV transition a value $> +0.27$ (we can exclude an appreciable M3 admixture). However, the measured A_2 value is

equal to -0.30 ± 0.02 . Thus $J^\pi(11.35) = 4^+$ is also excluded and the remaining possibilities are $J^\pi = 2^-$ or 3^\pm .

Further, the lifetime of the 4.88 MeV level (see table 2) limits the spin of this level to $J^\pi(4.88) = 2^\pm$, 3^\pm or 4^+ . A simultaneous least-squares fit of the parameters ρ_{20}/ρ_{00} , ρ_{40}/ρ_{00} , $x(6.47)$, $x(1.07)$ and $x(2.71)$ to the measured values of $A_2(6.47)$, $A_4(6.47)$, $A_2(1.07)$, $A_4(1.07)$, $A_2(2.71)$ and $A_4(2.71)$, with quadrupole admixtures exceeding 10 W.u. excluded, gives as a unique result $J(4.88) = 3$ for both $J(11.35) = 2$ and $J(11.35) = 3$.

The value of $\rho_{20}/\rho_{00} = -0.77$, found by this fitting procedure for $J(11.35) = 2$, combined with the results of the angular distribution measurement for the $11.35 \rightarrow 2.17$ MeV transition, involves for the latter an M2 strength of at least 10 W.u. This only leaves the possibilities $J^\pi(11.35) = 3^\pm$, with the following values for the statistical tensor ratios $\rho_{20}/\rho_{00} = -0.72 \pm 0.07$ and $\rho_{40}/\rho_{00} = 0.0 \pm 0.2$, which are in good agreement with the more accurate values found from the (p, α_0) work²⁾, $\rho_{20}/\rho_{00} = -0.70 \pm 0.01$ and $\rho_{40}/\rho_{00} = +0.01 \pm 0.01$.

Finally, the measured polarizations of the $4.88 \rightarrow 3.81$ MeV and $11.35 \rightarrow 4.88$ MeV transitions determine the parities of both the 4.88 and 11.35 MeV levels as odd.

Summary of results

$J^\pi(11.35) = 3^-$, $J^\pi(4.88) = 3^-$, $\rho_{20}/\rho_{00} = -0.72 \pm 0.07$, $\rho_{40}/\rho_{00} = 0.0 \pm 0.2$, $x(11.35 \rightarrow 4.88) = +0.16 \pm 0.10$, $x(4.88 \rightarrow 2.17) = -0.10 \pm 0.07$, $x(4.88 \rightarrow 3.81) = -0.03 \pm 0.07$.

3.4.3. *The $E_p = 1\,262$ keV resonance and the 4.57 MeV level.* As no angular distribution measurements were performed at the $E_p = 1\,262$ keV resonance, no definite conclusions could be drawn for the J^π -values of the 4.57 and 11.47 MeV levels. However, the observed decay and the lifetime of the 4.57 MeV level impose certain restrictions on the J^π values of both levels.

The resonance characteristics (E_p , E_x , strength and decay) are given in fig. 1. The decay proceeds 34 % via the $11.47 \rightarrow 4.57 \rightarrow 2.17$ MeV cascade and 41 % to the ground state.

The mean life of the 4.57 MeV level is measured at this resonance from the $E_\gamma = 2.40$ MeV ($4.57 \rightarrow 2.17$ MeV) transition and amounts to 48 ± 10 fs (see table 2). This life-time excludes pure quadrupole character for the 2.40 MeV γ -ray (E2 radiation would correspond to a strength of 28 W.u.) and therefore limits the spin of the 4.57 MeV level to $J = 1, 2$ or 3 .

The 4.57 MeV level is also fed at the $E_p = 1\,732$ keV, $J^\pi = 4^-$ resonance with a branching ratio of 2 %. The strength of this resonance excludes M2 character (corresponding to 29 W.u.) for the $11.93 \rightarrow 4.57$ MeV transition. The J^π of the 4.57 MeV level is therefore limited to $J^\pi = 2^-$ or 3^\pm . If one assumes that the strong transitions from the resonance level to the ground state and to the 4.57 MeV level have dipole character, one should conclude that the 4.57 MeV level has $J^\pi = (2^-)$.

As to the $E_p = 1\,262$ keV resonance level, the strong 11.47 MeV transition to the ground state suggests $J = 1$ for this level. A $J = 2$ assignment to this level involves a strength of 0.4 W.u. for even parity and of 10 W.u. for odd parity. This excludes $J^\pi(11.47) = 2^-$.

In the $^{37}\text{Cl}(p, \alpha_0)^{34}\text{S}$ reaction ²⁾, a resonance is reported at $E_p = 1\,263.5 \pm 1.4$ keV with $J^\pi = 1^-$ or 2^+ . If this resonance is the same as the (p, γ) resonance discussed above ($E_p = 1\,262.4 \pm 1.5$ keV), then the J^π value of the 11.47 MeV level is probably 1^- .

Summary of results

$J^\pi(11.47) = 1^\pm$ or 2^+ (probably 1^-),

$J^\pi(4.57) = 2^-$ or 3^\pm (probably 2^-).

3.4.4. The 6.67 MeV level. It is excited at the $E_p = 1\,089$ and $1\,094$ keV, $J^\pi = 5^-$ resonances with 4 % and 5 % branching ratios, respectively. It decays to the $E_x = 4.59$ MeV, $J^\pi = 5^-$, level.

The angular distribution of the $E_\gamma = 4.63$ MeV ($11.30 \rightarrow 6.67$ MeV) γ -ray is consistent with an unmixed $J = 5 \rightarrow 5$ transition. It is, however, also consistent with an unmixed $J = 5 \rightarrow 3$ or $5 \rightarrow 7$ transition.

The strength of the 1 094 keV resonance excludes pure M2 radiation (requiring at least 72 W.u.) for the $11.31 \rightarrow 6.67$ MeV transition. Therefore, the spin of the 6.67 MeV level has to be $J^\pi \geq 3$ with 3^+ excluded.

The fact that the 6.67 MeV level is excited at the $J^\pi = 5^-$ resonances and decays to a $J^\pi = 5^-$ state suggests that it also has $J^\pi = 5^-$ (see sect. 4).

Summary of results

$J(6.67) \geq 3$, 3^+ excluded, probably 5^- .

3.5. RADIATIVE WIDTHS

From the data given above, γ -transition strengths can be deduced.

The (p, γ) resonance strength $S = (2J+1)\Gamma_p\Gamma_\gamma/\Gamma$ gives for the radiative width of the resonance level $\Gamma_\gamma \geq S/(2J+1)$. In many cases Γ_γ will be close to this lower limit. However, the large Γ_α at the $E_p = 1\,138$ keV resonance will probably make the factor Γ_p/Γ at this resonance much smaller than unity. The partial radiative widths follow from the resonance branching ratios.

The radiative widths of the bound states are calculated from the measured lifetimes (subsect. 3.3).

The character and multipolarity of the γ -transitions are known from the spins and parities of the initial and final states and from the mixing ratios (see table 4). Therefore the transition strengths can be expressed in Weisskopf units $|M|^2 = \Gamma_\gamma/\Gamma_{\gamma w}$, where $\Gamma_{\gamma w}$ is the Weisskopf estimate ¹⁸⁾. For this estimate a nuclear radius $R = 1.2 A^{1/3}$ fm has been used.

The Weisskopf estimates for the various transitions are given in tables 5 and 6.

TABLE 4
Quadrupole/dipole amplitude mixing ratios

$E_p^a)$ (keV)	Transition (E_x in MeV)	$J^\pi_i \rightarrow J^\pi_f$	Mixing ratio x
<i>resonance levels</i>			
1 732	11.93 \rightarrow 6.60	$4^- \rightarrow 4^-$	-0.05 ± 0.08
	11.93 \rightarrow 6.21	$4^- \rightarrow 4^-$	$+0.02 \pm 0.08$
	11.93 \rightarrow 5.51	$4^- \rightarrow 3^{(-)}$	$+0.03 \pm 0.09$
	11.93 \rightarrow 4.59	$4^- \rightarrow 5^-$	$+0.20 \pm 0.10$
	11.93 \rightarrow 4.57	$4^- \rightarrow (2^-)$	∞
	11.93 \rightarrow 4.48	$4^- \rightarrow 4^-$	$+0.10 \pm 0.10$
1 138	11.35 \rightarrow 4.88	$3^- \rightarrow 3^-$	$+0.16 \pm 0.10$
	11.35 \rightarrow 3.81	$3^- \rightarrow 3^-$	$+0.20 \pm 0.10$
	11.35 \rightarrow 2.17	$3^- \rightarrow 2^+$	$+0.04 \pm 0.07$
1 094 ^{b)}	11.31 \rightarrow 5.66	$5^- \rightarrow 5^-$	$+0.13 \pm 0.06$
	11.31 \rightarrow 4.59	$5^- \rightarrow 5^-$	$+0.03 \pm 0.06$
1 089 ^{b)}	11.30 \rightarrow 5.66	$5^- \rightarrow 5^-$	$+0.19 \pm 0.06$
	11.30 \rightarrow 4.59	$5^- \rightarrow 5^-$	$+0.03 \pm 0.06$
<i>bound states</i>			
1 732	6.60 \rightarrow 4.48	$4^- \rightarrow 4^-$	$+0.05 \pm 0.08$
	6.21 \rightarrow 4.48	$4^- \rightarrow 4^-$	$+0.32 \pm 0.10$
1 138	4.88 \rightarrow 2.17	$3^- \rightarrow 2^+$	-0.10 ± 0.07
	4.88 \rightarrow 3.81	$3^- \rightarrow 3^-$	-0.03 ± 0.07
1 094 ^{b)} }	5.66 \rightarrow 4.59	$5^- \rightarrow 5^-$	$+0.10 \pm 0.09$
	3.81 \rightarrow 2.17	$3^- \rightarrow 2^+$	-0.01 ± 0.02
1 089 ^{b)} }	4.48 \rightarrow 3.81	$4^- \rightarrow 3^-$	-0.01 ± 0.02
	4.59 \rightarrow 3.81	$5^- \rightarrow 3^-$	∞
	4.59 \rightarrow 4.48	$5^- \rightarrow 4^-$	$+0.02 \pm 0.03$

^{a)} Proton energy of the resonance at which the transition is observed.

^{b)} Ref. ¹⁾.

TABLE 5
Transition strengths of γ -rays de-exciting $^{37}\text{Cl}(p, \gamma)^{38}\text{Ar}$ analogue levels

Transition (E_x in MeV)	$J^\pi_i, T_i \rightarrow J^\pi_f, T_f$	minimum $I_\gamma^a)$ (meV)	minimum strength in Weisskopf units $ M ^2 (\times 10^3)$		
			M1	E2 ^{b)}	E1
11.93 \rightarrow 6.60	$4^-, 2 \rightarrow 4^-, 1$	1 880	600		
11.93 \rightarrow 6.21	$4^-, 2 \rightarrow 4^-, 1$	1 250	320		
11.93 \rightarrow 5.51	$4^-, 2 \rightarrow 3^{(-)}, 1$	574	(110)		
11.93 \rightarrow 4.59	$4^-, 2 \rightarrow 5^-, 1$	365	45		
11.93 \rightarrow 4.57	$4^-, 2 \rightarrow (2^-), 1$	104		(790)	
11.93 \rightarrow 4.48	$4^-, 2 \rightarrow 4^-, 1$	365	42		
11.35 \rightarrow 4.88	$3^-, 2 \rightarrow 3^-, 1$	375	66		
11.35 \rightarrow 3.81	$3^-, 2 \rightarrow 3^-, 1$	188	20		
11.35 \rightarrow 2.17	$3^-, 2 \rightarrow 2^+, 1$	125			0.21
11.31 \rightarrow 5.66	$5^-, 2 \rightarrow 5^-, 1$	255	67	120	
11.31 \rightarrow 4.59	$5^-, 2 \rightarrow 5^-, 1$	337	53		
11.30 \rightarrow 5.66	$5^-, 2 \rightarrow 5^-, 1$	92	24	90	
11.30 \rightarrow 4.59	$5^-, 2 \rightarrow 5^-, 1$	181	28		

^{a)} Calculated from the resonance strengths (see subsect. 3.1) and the branchings given in fig. 4.

^{b)} The E2 strengths based on mixing ratios with an absolute value smaller than two times the standard error are not included. See table 4.

TABLE 6
Strengths of gamma transitions between bound states of ^{38}Ar

Transition (E_x in MeV)	$J^\pi_i, T_i \rightarrow J^\pi_f, T_f$	Γ_γ^a (meV)	Strength in Weisskopf units $ M ^2 (\times 10^3)$			
			M1	E2 ^{c)}	E1	E3
2.17 \rightarrow 0	$2^+, 1 \rightarrow 0^+, 1$	≤ 0.66		$\leq 2\ 300$		
3.38 \rightarrow 2.17	$0^+, 1 \rightarrow 2^+, 1$	≤ 1.3		$\leq 82\ 000$		
3.81 \rightarrow 0	$3^-, 1 \rightarrow 0^+, 1$	0.0035 ^{b)}				9 300
3.81 \rightarrow 2.17	$3^-, 1 \rightarrow 2^+, 1$	6.0			1.8	
3.94 \rightarrow 0	$(2)^+, 1 \rightarrow 0^+, 1$	6.3		(1 090)		
4.48 \rightarrow 3.81	$4^-, 1 \rightarrow 3^-, 1$	≤ 1.1	≤ 180			
4.57 \rightarrow 2.17	$(2^-), 1 \rightarrow 2^+, 1$	14			(1.3)	
4.59 \rightarrow 3.81	$5^-, 1 \rightarrow 3^-, 1$	≤ 0.13		$\leq 75\ 000$		
4.59 \rightarrow 4.48	$5^-, 1 \rightarrow 4^-, 1$	≤ 1.2	$\leq 50\ 000$			
4.88 \rightarrow 2.17	$3^-, 1 \rightarrow 2^+, 1$	8.4			0.55	
4.88 \rightarrow 3.81	$3^-, 1 \rightarrow 3^-, 1$	8.4	330			
5.66 \rightarrow 4.59	$5^-, 1 \rightarrow 5^-, 1$	10	400			
6.21 \rightarrow 4.48	$4^-, 1 \rightarrow 4^-, 1$	7.3	56	7 300		
6.60 \rightarrow 4.48	$4^-, 1 \rightarrow 4^-, 1$	26	130			

^{a)} Obtained from the lifetime measurements, see table 2.

^{b)} From $I_{3.81}/I_{1.64} = (5.8 \pm 0.8) \times 10^{-4}$, as given in ref. ²⁴⁾.

^{c)} The E2 strengths based on mixing ratios with an absolute value smaller than two times the standard error are not included. See table 4.

3.6. CONCLUSIONS

The excitation energies, lifetimes, spins and parities which follow from the present experiment, are summarized in table 7.

3.7. COULOMB-ENERGY DIFFERENCES AND THE ANALOGUE OF $^{38}\text{Cl}(0)$

The positions of the $J^\pi = 5^-, 3^-$ and 4^- states of ^{38}Ar at $E_x = 11.305, 11.351$ and 11.929 MeV, which are the analogues to the first three excited states of ^{38}Cl at $E_x = 0.671, 0.756$ and 1.314 MeV [ref. ¹⁹⁾], imply the following Coulomb-energy differences: $\Delta E_C = 6.500, 6.461$ and 6.481 MeV. No corrections were applied for the Thomas-Ehrman shift ²⁰⁾.

Taking $\Delta E_C = 6.48$ MeV, the expected position of the analogue of the ^{38}Cl ground state is at about $E_x = 10.62$ MeV, which corresponds to $E_p = 390$ keV. The expected resonance spin and parity are $J^\pi = 2^-$. From the $^{37}\text{Cl}(d, p)^{38}\text{Cl}$ reaction ¹⁹⁾, $l_n = 3$ is found for the ^{38}Cl ground state. However, a small $l_n = 1$ admixture cannot be excluded because the error in the angular distribution is large at the forward angles. Due to the low proton energy in the present experiment, the l_p value of the ground-state analogue resonance is expected to have mainly $l_p = 1$ with a small reduced proton width.

A very weak $^{37}\text{Cl}(p, \gamma)^{38}\text{Ar}$ resonance at $E_p = 427.1 \pm 0.5$ keV is reported in ref. ²¹⁾. The existence of this resonance was confirmed in the present work; the $2.17 \rightarrow 0$ MeV transition could be identified in the spectrum. Contaminant resonances, however, prevented the construction of a decay scheme.

TABLE 7
Properties of ^{88}Ar bound states

Present work			Previous work	
E_x (keV)	τ_m (fs)	J^π	$E_x^a)$ (keV)	$J^\pi^b)$
2 167.68 \pm 0.14	≥ 1000		2 170 \pm 5	2 ⁺
3 376.8 \pm 0.3	≥ 500		3 383 \pm 10	0 ⁺
3 810.0 \pm 0.2	110 \pm 80		3 816 \pm 10	3 ⁻
3 936.3 \pm 0.5	105 \pm 16		3 944 \pm 10	(2) ⁺
4 479.6 \pm 0.3	≥ 600		4 486 \pm 10	4 ⁻
4 565.9 \pm 0.5	48 \pm 10	(2 ⁻)	4 573 \pm 10	
4 585.0 \pm 0.5	≥ 500		4 594 \pm 10	5 ⁻
4 709.6 \pm 0.7			4 719 \pm 10	
4 877.0 \pm 0.3	39 \pm 13	3 ⁻	4 885 \pm 10	
5 083.2 \pm 1.7			5 093 \pm 10	
(5 155) ^{c)}			5 164 \pm 10	
(5 347) ^{c)}			5 357 \pm 10	
5 512.9 \pm 0.5	≥ 300	3 ⁽⁻⁾	5 522 \pm 10	
(5 551) ^{c)}			5 561 \pm 10	
5 591.0 \pm 2.0			5 603 \pm 10	
5 657.7 \pm 0.6	64 \pm 14		5 669 \pm 10	5 ⁻
(5 733) ^{c)}			5 743 \pm 10	
5 825.3 \pm 2.0			5 835 \pm 10	
5 853 \pm 3			5 869 \pm 10	
5 975.0 \pm 2.0			5 985 \pm 10	
(6 047) ^{c)}			6 058 \pm 10	
6 209.0 \pm 0.7	90 \pm 25	4 ⁻	6 222 \pm 10	
(6 248) ^{c)}			6 259 \pm 10	
6 269.4 \pm 2.0			6 286 \pm 10	
(6 335) ^{c)}			6 347 \pm 10	
6 352.5 \pm 2.0			6 360 \pm 20	
			6 420 \pm 20	
6 485.5 \pm 2.0			6 500 \pm 20	
			6 590 \pm 20	
6 601.2 \pm 0.4	25 \pm 7	4 ⁻	6 610 \pm 20	
			6 630 \pm 20	
6 673.3 \pm 1.5		(5 ⁻)	6 680 \pm 20	
			6 780 \pm 20	
			6 830 \pm 20	
			6 850 \pm 20	
			6 880 \pm 20	
6 902 \pm 3				

^{a)} As obtained from the $^{41}\text{K}(p, \alpha)^{88}\text{Ar}$ reaction ¹⁰⁾.

^{b)} As reviewed in ref. ²²⁾.

^{c)} Values from column 4 corrected for an energy-dependent systematic difference between the values in columns 1 and 4.

4. Discussion

4.1. COMPARISON OF THE ^{38}Ar LEVEL SCHEME WITH THEORETICAL CALCULATIONS

Shell-model calculations of the odd-parity levels in ^{38}Ar are given by Ern  ¹⁷⁾. In these calculations an inert ^{32}S core is assumed with a residual two-particle interaction of the outer nucleons in the $1d_{3/2}$ or $1f_{7/2}$ shells. Only one nucleon is considered to be in the $1f_{7/2}$ shell. The binding energies to the core and the two-particle matrix elements were obtained from a least-squares comparison with experimentally known levels.

These calculations are compared with the experimental results in table 8.

TABLE 8
Comparison of theoretical ¹⁷⁾ and experimental energy levels in ^{38}Ar

J^π	E_{exp} (MeV)	E_{th} (MeV)	Ref.
0^+	0	0	²²⁾
0^+	3.38	3.62 *)	²³⁾
2^+	2.17	1.96	²²⁾
0^-		6.97	
1^-		6.27, 7.21	
2^-	(4.57)	4.78, 5.67, 6.79, 7.60	this work
3^-	3.81	3.68	²²⁾
	4.88	4.89	this work
	(5.51)	6.65, 7.42, 7.67	this work
4^-	4.49	4.12	¹⁾
	6.21	6.08	this work
	6.60	6.53, 7.35, 7.83	this work
5^-	4.59	4.59	¹⁾
	5.67	5.51	¹⁾
	(6.67)	6.78, 7.57	this work
6^-		7.00, 7.40	
7^-		7.17	

*) Calculated with the assumptions (i) two nucleons in the $1f_{7/2}$ shell and (ii) the nucleons in the $1d_{3/2}$ as well as in the $1f_{7/2}$ shell are coupled to spin zero.

The positions of the levels at $E_x = 4.88$, 6.21 and 6.60 MeV found in the present work are in remarkable agreement with the theoretical predictions. The mean difference between the experimental and theoretical energies of these anti-analogue levels amounts to 70 keV.

Good agreement is found also between the experimental and theoretical positions of the levels at $E_x = 4.57$ and 6.67 MeV with probable $J^\pi = (2^-)$ and (5^-) assignments.

For the $J^\pi = 3^{(-)}$ level at $E_x = 5.51$ MeV, however, the agreement is poor. A possible explanation lies in the fact that the configuration of the 5.51 MeV state contains admixtures from other configurations (for instance $2p_{3/2}$) which are neglected

in the above calculations. Another explanation might be that the 5.51 MeV level has $J^\pi = 3^+$. As in a $(2s_{\frac{1}{2}}^n 1d_{\frac{3}{2}}^{10-n})$ configuration a $J^\pi = 3^+$, $T = 1$ combination is not possible, the simplest configurations to be expected are then $(d_{\frac{3}{2}}^{-4} f_{\frac{7}{2}}^2)$ or $(d_{\frac{3}{2}}^{-1} s_{\frac{1}{2}}^4 d_{\frac{3}{2}}^{-1})$.

4.2. THE M1 $J \rightarrow J$ ENHANCEMENT IN THE DECAY OF THE ANALOGUE STATES

The 5^- , 3^- and 4^- resonances of ^{38}Ar show all the features expected from analogue states of the first three ^{38}Cl levels if we assume that they correspond to the configurations mentioned in subsect. 4.1. They are very strong in comparison with neighbouring $T = 1$ resonances (see e.g. fig. 3) and a typical preference exists for γ -decay to bound "anti-analogue" states with the same spin and parity but with isospin $T = 1$. Moreover, these M1 $J \rightarrow J$ transitions are about an order of magnitude stronger than the $J \rightarrow J \pm 1$ transitions as already observed for the $J^\pi = 5^-$ analogue state by Ern  ¹⁾.

This enhancement of the M1 $J \rightarrow J$ transitions has been explained by Ern  ¹⁾ from the above mentioned shell-model calculations of the odd-parity levels. The main components of the configurations of the odd-parity levels with spin J and isospin T would be $|(1d_{\frac{3}{2}})jt, 1f_{\frac{7}{2}}; JT\rangle$. Here the five nucleons in the $1d_{\frac{3}{2}}$ shell are coupled to $j = \frac{3}{2}$ with isospin $t = \frac{1}{2}$ or $\frac{3}{2}$. If the dominant part of the M1 operator operates on the particle in the $1f_{\frac{7}{2}}$ shell, the dependence of the transition strength on the initial spin J_i and the final spin J_f is expressed by the factor ¹⁾

$$(2J_i + 1)(2J_f + 1) \left(\begin{matrix} J_i & J_f & 1 \\ \frac{7}{2} & \frac{7}{2} & \frac{3}{2} \end{matrix} \right)^2.$$

This factor favours $J_i \rightarrow J_f = J_i$ transitions over $J_i \rightarrow J_f = J_i \pm 1$ transitions, the preference being more pronounced for higher J -values as shown in table 9.

TABLE 9

Comparison of the theoretical ¹⁷⁾ and experimental branching ratios in the decay of the analogue states

J^π_i	J^π_f	Reduced intensities (I_γ/E_γ^3)	
		theoretical	measured ^{a)}
3^-	2^-	13.4	5 ± 2
	3^-	100	100 ± 8
	4^-	17.9	26 ± 7
4^-	3^-	13.0	15 ± 2
	4^-	100	100 ± 7
	5^-	10.0	9 ± 2
5^-	4^-	7.1	18 ± 4
	5^-	100	100 ± 7

^{a)} The transitions to the levels at $E_x = 4.57$, 5.51 and 6.67 MeV with the spin and parity assignments $J^\pi = (2^-)$, $3^{(-)}$ and (5^-) , respectively, are also included.

In order to better understand the measured lifetimes and transition probabilities, shell-model calculations taking into account more configurations than used in previous work are being carried out.

It is a pleasure to acknowledge Professor P. M. Endt's stimulating interest in this investigation. Thanks are also due to Professor A. M. Hoogenboom and P. de Wit who constructed the electronics for the Ge(Li) detector assembly. The assistance of C. Alderliesten, J. W. Waanders, M. W. Ockeloen and H. S. Pruys in measurements and calculations is gratefully acknowledged.

One of us (H. L.) wishes to express his gratitude for the cordial hospitality extended to him at the Physics Department of Utrecht University.

This investigation was partly supported by the joint program of the "Stichting voor Fundamenteel Onderzoek der Materie" and the "Nederlandse Organisatie voor Zuiver Wetenschappelijk Onderzoek".

References

- 1) F. C. Ern , W. A. M. Veltman and J. A. M. Wintermans, *Nuclear Physics* **88** (1966) 1
- 2) B. Bošnjakovi , J. A. van Best and J. Bouwmeester, *Nuclear Physics* **A94** (1967) 625
- 3) H. Van Rinsvelt and P. B. Smith, *Physica* **30** (1964) 59
- 4) P. H. Vuister, *Nuclear Physics* **83** (1966) 593
- 5) C. van der Leun, D. M. Sheppard and P. M. Endt, *Nuclear Physics* **A100** (1967) 316
- 6) M. Suffert, P. M. Endt and A. M. Hoogenboom, *Physica* **25** (1959) 659
- 7) G. A. P. Engelbertink and P. M. Endt, *Nuclear Physics* **88** (1966) 12
- 8) J. B. Marion, *Phys. Lett.* **21** (1966) 61
- 9) J. B. Marion, University of Maryland Report ORO-2098-58 (revised) (Aug. 1967)
- 10) R. G. Allas, L. Meyer-Sch tzmeister and D. von Ehrenstein, *Nuclear Physics* **61** (1965) 289
- 11) J. H. Mattauch, W. Thiele and A. H. Wapstra, *Nuclear Physics* **67** (1965) 1
- 12) J. Lindhard, M. Scharff and H. E. Schi tt, *Mat. Fys. Medd. Dan. Vid. Selsk.* **33**, No. 14 (1963)
- 13) A. E. Blaugrund, *Nuclear Physics* **88** (1966) 501
- 14) J. H. Ormrod, J. R. Macdonald and H. E. Duckworth, *Can. J. Phys.* **43** (1965) 275
- 15) W. Bruynesteyn, (Utrecht), private communication
- 16) F. C. Ern , *Nuclear Physics* **84** (1966) 241
- 17) F. C. Ern , *Nuclear Physics* **84** (1966) 91
- 18) V. F. Weisskopf, *Phys. Rev.* **83** (1951) 1073
- 19) J. Rapaport and W. W. Buechner, *Nuclear Physics* **83** (1966) 80
- 20) R. G. Thomas, *Phys. Rev.* **88** (1952) 1109
- 21) M. Heitzmann and S. Wagner, *Z. Naturf.* **16a** (1961) 1136
- 22) P. M. Endt and C. van der Leun, *Nuclear Physics* **A105** (1967) 1
- 23) C. A. Whitten, *Bull. Am. Phys. Soc.* **10** (1965) 121
- 24) B. L. Robinson, *Phys. Rev.* **140** (1965) 1529